TLR-Independent and P2X7-Dependent Signaling Mediate *Alu* RNA-Induced NLRP3 Inflammasome Activation in Geographic Atrophy

Nagaraj Kerur,[1] Yoshio Hirano,[1] Valeria Tarallo,[1,5] Benjamin J. Fowler,[1,4] Ana Bastos-Carvalho,[1] Tetsuhiro Yasuma,[1] Reo Yasuma,[1] Younghee Kim,[1] David R. Hinton,[6] Carsten J. Kirschning,[7] Bradley D. Gelfand,[1–3] and Jayakrishna Ambati[1,4]

[1]Department of Ophthalmology and Visual Sciences, University of Kentucky, Lexington, Kentucky
[2]Department of Biomedical Engineering, University of Kentucky, Lexington, Kentucky
[3]Department of Microbiology, Immunology, and Human Genetics, University of Kentucky, Lexington, Kentucky
[4]Department of Physiology, University of Kentucky, Lexington, Kentucky
[5]Angiogenesis Lab, Institute of Genetics and Biophysics, CNR, Naples, Italy
[6]Departments of Pathology and Ophthalmology, Keck School of Medicine of the University of Southern California, Los Angeles, California
[7]Institute of Medical Microbiology, University of Duisburg-Essen, Essen, Germany

Correspondence: Jayakrishna Ambati, Ophthalmology and Visual Sciences, University of Kentucky, 740 S. Limestone Street, Suite C-300 Lexington, KY 40536; jamba2@email.uky.edu.

NK and YH contributed equally to the work presented here and should therefore be regarded as equivalent authors.

Submitted: May 28, 2013
Accepted: October 2, 2013

Citation: Kerur N, Hirano Y, Tarallo V, et al. TLR-independent and P2X7-dependent signaling mediate *Alu* RNA-induced NLRP3 inflammasome activation in geographic atrophy. *Invest Ophthalmol Vis Sci*. 2013;54:7395–7401. DOI:10.1167/iovs.13-12500

Purpose. Accumulation of *Alu* RNA transcripts due to DICER1 deficiency in the retinal pigmented epithelium (RPE) promotes geographic atrophy. Recently we showed that *Alu* RNA activated the NLRP3 inflammasome, leading to RPE cell death via interleukin-18 (IL-18)-mediated MyD88 signaling. However, the molecular basis for NLRP3 inflammasome activation by *Alu* RNA is not well understood. We sought to decipher the key signaling events triggered by *Alu* RNA that lead to priming and activation of the NLRP3 inflammasome and, ultimately, to RPE degeneration by investigating the roles of the purinoreceptor P2X7, the transcription factor NF-κB, and the Toll-like receptors (TLRs) in these processes.

Methods. Human and mouse RPE cells were transfected with a plasmid encoding an *Alu* element (pAlu) or an in vitro-transcribed *Alu* RNA. Inflammasome priming was assessed by measuring *NLRP3* and *IL18* mRNA levels by real-time quantitative PCR. Using immunoblotting, we assessed NF-κB activation by monitoring phosphorylation of its p65 subunit, and inflammasome activation by monitoring caspase-1 cleavage into its active form. RPE degeneration was induced in mice by subretinal transfection of pAlu or *Alu* RNA. The NF-κB inhibitor BAY 11-7082, the P2X7 receptor antagonist A-740003, and the NLRP3 inflammasome inhibitor glyburide were delivered by intravitreous injections. We studied wild-type (WT) C57Bl/6J, *P2rx7*$^{-/-}$, *Nfkb1*$^{-/-}$, and *Tlr23479*$^{-/-}$ mice. RPE degeneration was assessed by fundus photography and zonula occludens-1 (ZO-1) staining of mouse RPE.

Results. *Alu* RNA-induced NF-κB activation, independent of TLR-1, -2, -3, -4, -6, -7, and -9 signaling, was required for priming the NLRP3 inflammasome. *Nfkb1*$^{-/-}$ and *P2rx7*$^{-/-}$ mice and WT mice treated with the pharmacological inhibitors of NF-κB, P2X7, or NLRP3, were protected against *Alu* RNA-induced RPE degeneration.

Conclusions. NF-κB and P2X7 are critical signaling intermediates in *Alu* RNA-induced inflammasome priming and RPE degeneration. These molecules are novel targets for rational drug development for geographic atrophy.

Keywords: AMD, inflammasome, NLRP3

Geographic atrophy (GA) is an advanced form of age-related macular degeneration characterized by central loss of vision due to confluent areas of retinal pigmented epithelium (RPE) loss and overlying photoreceptor degeneration.[1–3] To date, there is no approved therapy available for this disease, due largely to lack of clear understanding of its molecular pathogenesis. Recently, we showed that the microRNA (miRNA) processing enzyme DICER1 is specifically reduced in the RPE of GA eyes. The reduced DICER1 levels in the RPE result in an increased abundance of *Alu* RNA transcripts, which in turn promotes RPE cell death.[4,5] Under healthy conditions, DICER1-mediated enzymatic processing metabolizes these *Alu* RNAs into innocuous cleavage fragments; consequently a deficit in DICER1 abundance results in an increased accumulation of toxic *Alu* RNA transcripts and RPE degeneration.[4]

Alu RNAs are noncoding transcripts belonging to the *Alu* family of retrotransposons, an abundant repetitive DNA sequence in the human genome. Typically, *Alu* RNA is an ~300 nucleotide (nt) transcript with a double-stranded dimeric secondary structure consisting of right and left arms separated by an A-rich linker.[6] Accumulation of these noncoding *Alu* RNA transcripts due to DICER1 deficiency induced human RPE cell

death and RPE degeneration in mice.[4] More recent studies identified that *Alu* RNA cytotoxicity in RPE is mediated by activation of the inflammasome NLRP3 and ensuing interleukin-18 (IL-18) and MyD88 signaling.[5]

NLRP3, an intracellular pattern recognition receptor (PRR) of the nod-like receptor (NLR) family forms large multiprotein complexes called inflammasomes. A diverse class of signals including cytosolic DNA, RNA, bacteria, and viruses stimulates the NLRP3 inflammasome leading to activation of caspase-1 and secretion of IL-18 and IL-1β.[7,8] NLRP3 inflammasome activation models posit the requirement of at least two signals, "priming" and "activation" (Fig. 1A). Priming involves the upregulation of the inflammasome gene expression via various transcriptionally active signaling receptors; activation involves assembly of a multiprotein inflammasome complex and proteolytic processing of caspase-1, IL-18, and IL-1β.[7,8]

Priming of the NLRP3 inflammasome is regulated by NF-κB activation by various proinflammatory signals emanating from Toll-like receptor (TLR) activation and production of reactive oxygen species (ROS).[6,8] The mechanisms regulating the activation step of the NLRP3 inflammasome are ambiguous, although it is clear that P2X7 and ROS are major contributors to this process in multiple systems.[7,8] Also it is clear that there is an interplay between P2X7 and ROS processes; for example, P2X7 signaling leads to ROS generation-dependent inflammasome priming.[9–11] Interestingly, as we demonstrated, *Alu* RNA activation of the NLRP3 inflammasome occurred via ROS intermediates.[5] Therefore, we investigated whether P2X7 signaling was also involved in *Alu* RNA-induced inflammasome activation.

Here, we demonstrate that NF-κB signaling and P2X7 activation play key roles in *Alu* RNA-induced inflammasome priming and activation and RPE degeneration. We also show that *Alu* RNA-induced NF-κB activation is independent of TLR signaling, suggesting sensing of *Alu* RNA by an unknown intracellular pattern recognition receptor.

Materials and Methods

Mice

All animal experiments were approved by institutional review committees and carried out in accordance with the Association for Research in Vision and Ophthalmology Statement for the Use of Animals in Ophthalmic and Visual Research. Wild-type (WT) C57BL/6J, *Nfkb1*$^{-/-}$ (C57BL/6J mice backcrossed for 12 generations), and *P2rx7*$^{-/-}$ (C57BL/6J mice backcrossed for 7 generations) mice were purchased from Jackson Laboratory (Bar Harbor, ME). "Quintuple knockout" mice simultaneously deficient for TLR2, TLR3, TLR4, TLR7, and TLR9 (*Tlr23479*$^{-/-}$ mice, C57BL/6J, backcrossed for 10 generations) have been previously described.[12] For all procedures, anesthesia was achieved by intraperitoneal injection of 100 mg/kg ketamine hydrochloride (Ft. Dodge Animal Health) and 10 mg/kg xylazine (Phoenix Scientific), and pupils were dilated with topical 1% tropicamide (Alcon Laboratories).

Fundus Photography

Retinal photographs of dilated mouse eyes were taken with a model TRC-50 IX camera (Topcon) linked to a digital imaging system (Sony).

Subretinal Injection

Subretinal injections (1 μL) in mice were given using a Pico-Injector (PLI-100; Harvard Apparatus). In vivo transfection of plasmids encoding *Alu* sequences (pAlu) or empty control vector (pNull) was carried out by using a DNA transfection reagent (10% NeuroPORTER; Genlantis) as previously described.[4,5,13,14] In vitro-transcribed *Alu* RNA (0.3 μg/μL) was injected as described earlier.[4,5]

Drug Treatments

Glyburide, glipizide (Sigma-Aldrich), and P2X7 inhibitors (Santa Cruz Biotechnology) dissolved in PBS or dimethyl sulfoxide (DMSO) were injected into the vitreous humor in a total volume of 1 μL with a 33-gauge microsyringe (Exmire; Ito Corp.). WT mice received the inhibitors or vehicle delivered into the vitreous 24 hours before and again 72 hours after exposure to *Alu* RNA.

Assessment of RPE Degeneration

Alu RNA-mediated RPE degeneration was induced by exposing mice to *Alu* RNA via subretinal injection of a plasmid encoding an *Alu* element (pAlu) (or a control plasmid) or an in vitro-transcribed *Alu* RNA.[4,5] Seven days later, RPE health was assessed by fundus photography and immunofluorescence staining of zonula occludens-1 (ZO-1) on RPE flat mounts (whole mount of posterior eye cup containing RPE and choroid layers). Mouse RPE/choroid flat mounts were fixed with 4% paraformaldehyde or 100% methanol, stained with rabbit polyclonal antibodies against mouse ZO-1 (1:100, Invitrogen) and visualized with Alexa594 (Invitrogen). All images were obtained by microscopy (model SP-5, Leica; or Axio Observer Z1, Zeiss).

Cell Culture

All cells were maintained at 37°C in a 5% CO_2 environment. Primary mouse and human fetal RPE cells were isolated as previously described.[15,16] Primary mouse RPE cells were isolated from 6- to 8-week-old WT C57BL/6J mice. Mouse RPE samples were maintained in Dulbecco modified Eagle medium (DMEM) supplemented with 20% fetal bovine serum (FBS) and standard antibiotics concentrations, and primary human RPE cells were maintained in DMEM supplemented with 10% FBS and antibiotics. For examining the role of NF-κB in NLRP3 priming, we preincubated the specific NF-κB inhibitor Bay 11-7082 (Sigma-Aldrich) for 1 hour with RPE cells before stimulating them with *Alu* RNA.

In Vitro Transcription of *Alu* RNAs

T7 promoter containing *Alu* expression plasmid was linearized and used for making in vitro–transcribed *Alu* RNA by using an in vitro transcription kit (T7-Flash transcription kit; AmpliScribe; Epicenter) following the manufacturer's instructions. The resulting *Alu* RNA was treated with DNase and purified (MEGAclear; Ambion), and integrity was monitored by gel electrophoresis.

Transient Transfection

Human or mouse RPE cells were transfected with pNull, pAlu, or in vitro–transcribed *Alu* RNA by using Lipofectamine 2000 (Invitrogen) following the manufacturer's instructions.

Western Blotting

Cells lysed in radioimmunoprecipitation assay (Sigma-Aldrich) lysis buffer supplemented with protease cocktail inhibitor were homogenized by sonication. Protein concentrations were determined using a Bradford assay kit (Bio-Rad) with bovine

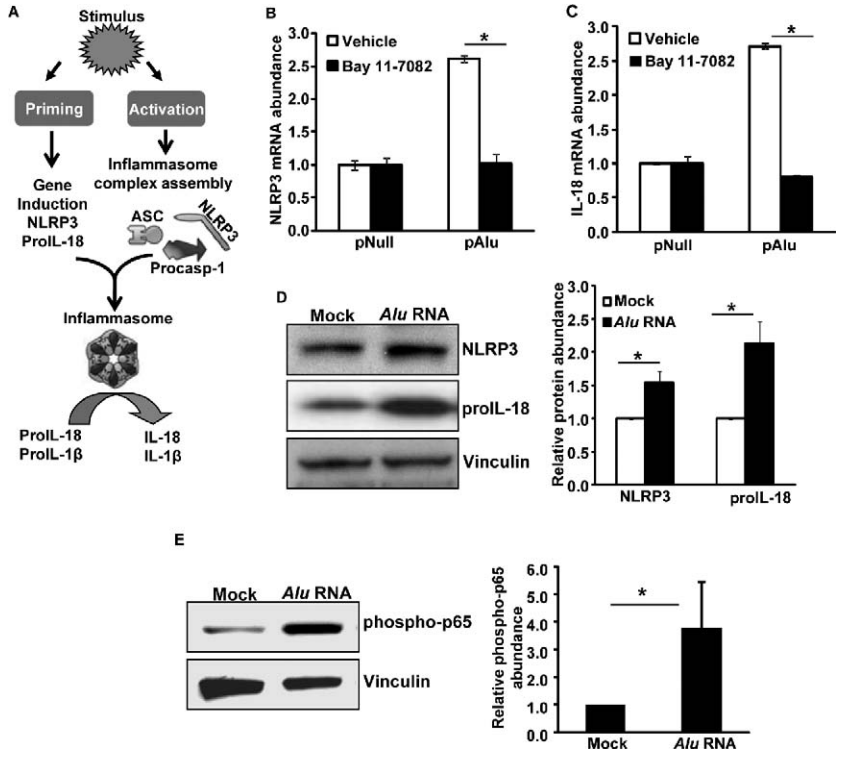

FIGURE 1. (**A**) Two-signal model of the NLRP3 inflammasome is shown: NLRP3 activation requires two signals called "priming" and "activation." Priming involves induction of inflammasome genes (NLRP3, IL-18, and IL-1β), and activation involves the assembly of a multiprotein scaffold consisting of NLRP3, ASC, and pro-caspase-1, which executes the proteolytic activation of caspase-1. Subsequently, the activated caspase-1 cleaves pro-IL-18 and pro-IL-1β into mature cytokines. Human RPE cells preincubated with vehicle (DMSO) or the NF-κB inhibitor Bay 11-7082 (20 μM) were exposed to *Alu* RNA via transfection of a plasmid encoding *Alu* RNA (pAlu) or an empty vector control plasmid (pNull). *Alu* RNA-induced priming of NLRP3 was assessed by real-time qPCR for (**B**) NLRP3 mRNA abundance and (**C**) IL-18 mRNA abundance. $n = 3$. (**D**) Protein levels of NLRP3 and IL-18 were induced in human RPE cells exposed to *Alu* RNA; *right panel* shows densitometric quantification of the bands on the immunoblot. (**E**) NF-κB is activated (phospho p65) in human RPE cells exposed to *Alu* RNA; *bar chart* shows densitometric quantification of the immunoreactive phospho p65 bands. Gene expression results are expressed as means ± SEM, with $P < 0.05$ considered statistically significant. *n* represents the number of experiments from which the data was obtained. Representative immunoblots from 3 independent experiments are shown.

serum albumin as a standard. Equal amounts of protein samples (20–40 μg) prepared in Laemmli buffer were resolved by SDS-PAGE on Tris-glycine gels (Novex; Invitrogen) and transferred onto polyvinylidene difluoride membranes (Immun-Blot; Bio-Rad). The transferred membranes were blocked for 1 hour at room temperature and incubated with antibodies against caspase-1 (1:1000 dilution; Invitrogen), IL-18 (1:1000 dilution; MBL International), NLRP3 (1:1000 dilution; Enzo Life Sciences) and NF-κB (1:1000; Cell Signaling) at 4°C overnight. Immunoreactive bands were developed by enhanced chemiluminescence reaction. Band intensities on the immunoblots were quantified using ImageJ software (National Institutes of Health).

Real-Time PCR

Human/mouse RPE cells were exposed to *Alu* RNA via transfection of a plasmid encoding an *Alu* element (pAlu); 24 hours later, we analyzed inflammasome priming by examining the mRNA levels of pro-IL-18 and NLRP3 by using real-time quantitative RT-PCR (RT-qPCR). Total RNA was extracted from cells using TRIzol reagent (Invitrogen) following the manufacturer's instructions. An equal quantity of DNase-treated RNA was reverse transcribed using a reverse transcription kit (QuantiTect; Qiagen). The RT products (cDNA) were amplified by real-time qPCR (7900 HT Fast real-time PCR system; Applied Biosystems) with SYBR Green detection system. At the end of amplification, melting curve analysis was applied using the dissociation protocol from the sequence detection system to exclude contamination with nonspecific PCR products. For negative controls, no RT products were used as templates in the qPCR. Relative expressions of target genes were determined by the 2^{-DDCt} method using the 18S rRNA housekeeping gene. Oligonucleotide primers specific for human *IL18* (forward, 5′-ATCACTTGCACTCCGGAGGTA-3′, and reverse, 5′-AGAGCG CAATGGTGCAATC-3′), human *NLRP3* (forward, 5′-GCACCTGTTGTGCAATCTGAA-3′, and reverse, 5′-TCCTGA CAACATGCTGATGTGA-3′), human 18S rRNA (forward, 5′-CGCAGC TAGGAATAATGGAATAGG-3′, and reverse, 5′-GCCTCAGTTCCGAAAACCAA-3′), mouse Nlrp3 (forward, 5′-ATGCTGCTTCGACATCTCCT-3′, and reverse, 5′-AACCAATGC GAGATCCTGAC-3′), mouse *Il18* (forward, 5′-GA CAGCCTGTGTT CGAGGAT-3′, and reverse, 5′-TGGATC CATTTCCTCAAAGG-3′), and mouse 18S rRNA (forward, 5′-TTCGTATTGCGCCGCTAGA-3′, and reverse, 5′-CTTTCGCTCTGGTCCGTCTT-3′) were used.

Statistical Analyses

Real-time RT-qPCR gene expression results and immunoblot densitometry values expressed as means ± standard error of the mean (SEM) were analyzed using two-tailed Student's *t*-test. The binary readouts of RPE degeneration (i.e., presence or

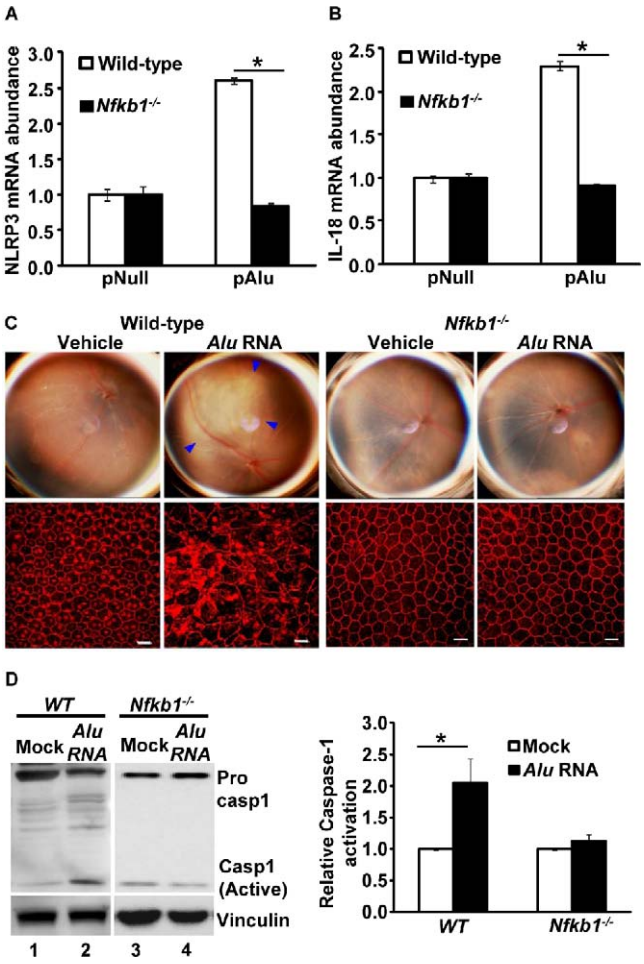

FIGURE 2. Priming of NLRP3 was analyzed by examining the mRNA abundance of (**A**) NLRP3 and (**B**) IL-18 in WT and *Nfkb1*$^{-/-}$ mouse RPE cells transfected with pAlu or empty vector (pNull). $n = 8$. (**C**) *Alu* RNA causes RPE degeneration in WT mice but not in *Nfkb1*$^{-/-}$ mice: WT and *Nfkb1*$^{-/-}$ mice were exposed to *Alu* RNA by subretinal injection. $n = 8$. *Alu* RNA-induced RPE degeneration was assessed by fundus examination and ZO-1 staining of RPE flat mount. Disrupted RPE cell boundaries shown by ZO-1 staining of RPE flat mounts indicate RPE degeneration. *Blue arrowheads* in the fundus picture indicate areas of RPE degeneration ($P = 0.0002$, χ^2 test). (**D**) WT and *Nfkb1*$^{-/-}$mouse RPE cells were exposed to *Alu* RNA, and NLRP3 activation was assessed by examining the activation of caspase-1 by Western blotting; the densitometric quantification of active caspase-1 (p20) bands in the immunoblots is presented in the bar graph.

absence of RPE degeneration on fundus and ZO-1-stained flat mount images) were analyzed using χ^2 test. P values < 0.05 were deemed statistically significant.

RESULTS

NF-κB Mediates *Alu* RNA-Induced Inflammasome Priming

Recently, we demonstrated that *Alu* RNA accumulation due to DICER1 deficiency induced human RPE cell death and RPE degeneration in mice through activation of caspase-1 via NLRP3 inflammasome activation.[5] Activation of NLRP3 requires a priming signal to induce adequate levels of NLRP3, IL-18, and IL-1β and an activating signal to promote assembly of an inflammasome multiprotein complex.[7,8] In most cases, priming is initiated by activation of additional pattern recognition receptors such as TLRs or through inflammatory cytokines. Importantly, these diverse signaling events converge to activate NF-κB transcription factors. The NF-κB family of transcription factors regulates many cellular responses including inflammation and cell death. Here we examined whether NF-κB signaling is critical for *Alu* RNA-induced inflammasome priming and RPE degeneration. The expression of *Alu* RNA through transfection of an *Alu* expression plasmid (pAlu) induced priming of the NLRP3 inflammasome as indicated by induction of the NLRP3 (Fig. 1B) and IL-18 genes (Fig. 1C). In support of gene expression data, human RPE cells exposed to *Alu* RNA also showed an increased abundance of pro-IL-18 and NLRP3 proteins (Fig. 1D). Furthermore *Alu* RNA-induced NLRP3 inflammasome priming was suppressed by an NF-κB inhibitor (Bay 11-7082) (Figs. 1B, 1C). In support of these findings, immunoblotting of protein lysates of human RPE cells exposed to *Alu* RNA also demonstrated activation of NF-κB, as indicated by increased phosphorylation of its p65 subunit (Fig. 1E). Furthermore, *Alu* RNA did not induce priming of the NLRP3 inflammasome in RPE cells isolated from *Nfkb1*$^{-/-}$ mice (Figs. 2A, 2B). Taken together, these findings implicate NF-κB as the key transcription factor regulating *Alu* RNA-induced NLRP3 inflammasome priming.

NF-κB-Mediated Signaling Is Required For *Alu* RNA-Induced RPE Degeneration

Our cell culture studies with genetic and pharmacological approaches suggested that NF-κB is critical in regulating NLRP3 inflammasome priming. Next, using *Nfkb1*$^{-/-}$ mice, we tested the role of NF-κB in mediating *Alu* RNA-induced mouse RPE degeneration. Recently we established a model for in vivo testing of *Alu* RNA-induced RPE degeneration[4,5] by subretinal delivery of *Alu* RNA expression plasmid (pAlu) or of in vitro-transcribed *Alu* RNA. Whereas *Alu* RNA induced RPE degeneration in WT mice, it did not do so in *Nfkb1*$^{-/-}$ mice (Fig. 2C). To further confirm our rationale that loss of *Alu* RNA-induced RPE degeneration in *Nfkb1*$^{-/-}$ mice was indeed due to impaired NLRP3 activation in the absence NF-κB-mediated priming signals, we assessed the ability of *Alu* RNA to induce caspase-1 activation in *Nfkb1*$^{-/-}$ mouse RPE cells. As anticipated, *Alu* RNA was unable to activate caspase-1 in *Nfkb1*$^{-/-}$ mouse RPE cells (Fig. 2D, compare active casp1 in lane 3 versus that in lane 4) compared to marked caspase-1 activation in WT RPE cells (Fig. 2D, compare active casp1 in lane 1 versus that in lane 2). Collectively, these findings demonstrate that intact NF-κB signaling is a critical regulatory checkpoint in the *Alu* RNA-induced inflammasome activation and RPE degeneration.

Alu RNA-Induced NF-κB Activation and Inflammasome Priming Are Independent of TLR Signaling

Because *Alu* RNA-induced NLRP3 inflammasome activation and RPE degeneration were regulated by NF-κB, we next examined the upstream signaling pathways involved in mediating these events. TLRs are an important set of cellular PRRs that detect various structural motifs, including intracellular double-stranded RNA (dsRNA).[17] We tested whether *Alu* RNA, with its double-stranded dimeric secondary structure, activates TLR signaling leading to NF-κB-mediated priming of the NLRP3 inflammasome. To answer this question, we examined activation of NF-κB and inflammasome priming in *Tlr23479*$^{-/-}$ mouse RPE cells. Surprisingly, NF-κB activation following *Alu* RNA treatment persisted in TLR signaling-

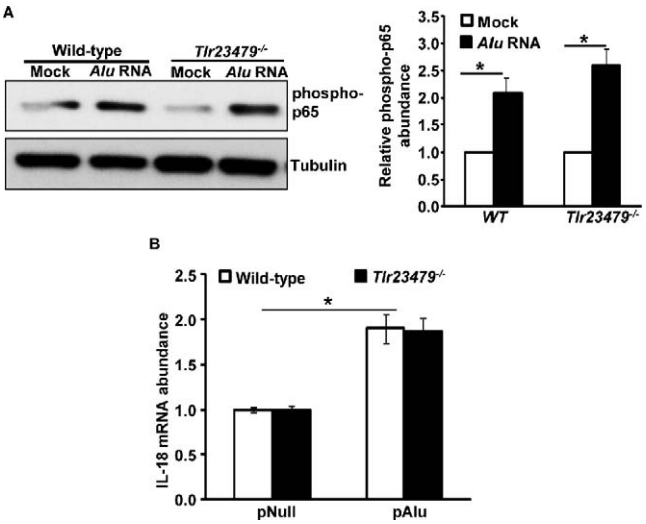

FIGURE 3. (**A**) *Alu* RNA-induced NF-κB activation is independent of signaling via TLR2/3/4/7/9; bar chart at *right* shows densitometric quantification of the phospho p65 bands on the immunoblot. (**B**) *Alu* RNA-induced induction of the IL-18 gene is independent of TLR2/3/4/7/9 signaling. A representative immunoblot from three independent experiments is shown.

deficient mice (Fig. 3A). Corroborating these data, induction of the IL-18 gene in mice lacking multiple TLRs (*Tlr23479*$^{-/-}$ mice) was similar to that in WT mice (Fig. 3B). Collectively, these findings demonstrate that *Alu* RNA-induced NF-κB activation and NLRP3 inflammasome priming occur in a manner independent of TLR activation, suggesting the existence of noncanonical, TLR-independent NF-κB activation and priming of the NLRP3 inflammasome.

P2X7 Mediates *Alu* RNA-Induced RPE Degeneration/Inflammasome Activation

NLRP3 inflammasome induction is tightly regulated, with multiple signaling pathways controlling priming and assembly of the multiprotein inflammasome complex. Although the signaling pathways regulating priming are well understood, pathways orchestrating the assembly of the multiprotein complex leading to caspase-1 activation remain nebulous. We tested whether P2X7, a well-known inflammasome activator in other systems, is critical for *Alu* RNA-induced activation of the NLRP3 inflammasome and RPE degeneration. RPE cells isolated from WT and *P2rx7*$^{-/-}$ mice were transfected with *Alu* RNA, and activation of caspase-1 was assessed by immunoblotting. *Alu* RNA induced the proteolytic cleavage of pro-caspase-1 into its active p20 subunit in WT mouse RPE (mRPE) cells (Fig. 4A, compare lanes 1 and 2) but not in *P2rx7*$^{-/-}$ mouse RPE cells

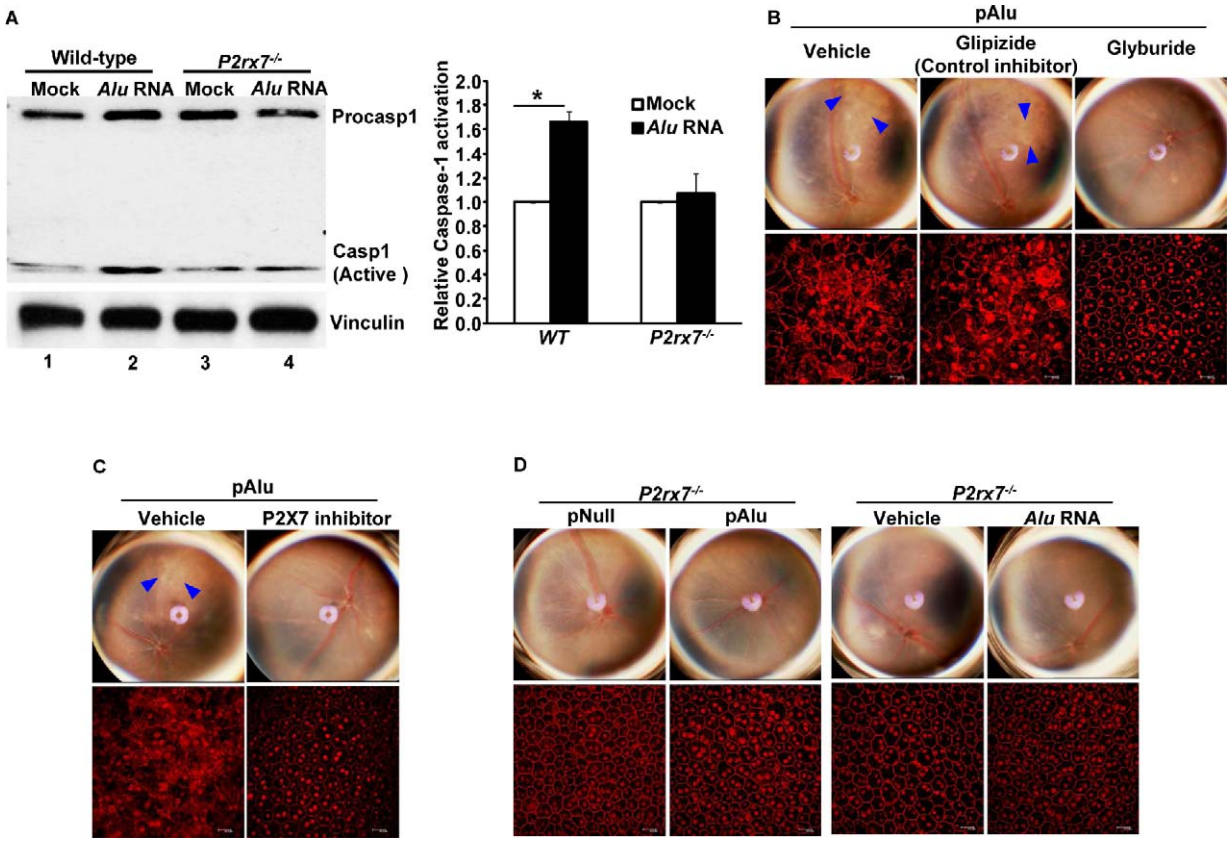

FIGURE 4. (**A**) WT and *P2rx7*$^{-/-}$ mouse RPE cells were exposed to *Alu* RNA, and NLRP3 activation was assessed by examining the activation of caspase-1 by Western blotting; densitometric quantification of active caspase-1 (p20) bands in the immunoblot is shown in the bar graph. (**B**) The NLRP3 inflammasome inhibitor glyburide, which acts downstream of P2X7 receptors, suppressed *Alu* RNA-induced RPE degeneration in mice. The structurally similar control inhibitor glipizide, which is not an inhibitor of NLRP3, did not suppress *Alu* RNA-induced RPE degeneration. $n = 12$ ($P = 0.0001$, χ^2 test). (**C**) The P2X7 inhibitor suppressed *Alu* RNA (pAlu)-induced RPE degeneration in WT mice. $n = 8$ ($P = 0.0001$, χ^2 test). (**D**) P2X7-deficient mice are not susceptible to *Alu* RNA-induced RPE degeneration. $n = 8$ ($P = 0.0001$, χ^2 test). Immunoblots shown in the figure are representative of 3 independent experiments. *Blue arrowheads* in the fundus picture indicate areas of RPE degeneration. The fundus and ZO-1-stained flat mount images were statistically analyzed using the χ^2 test. *n* represents the number of experiments or animals from which the data was obtained.

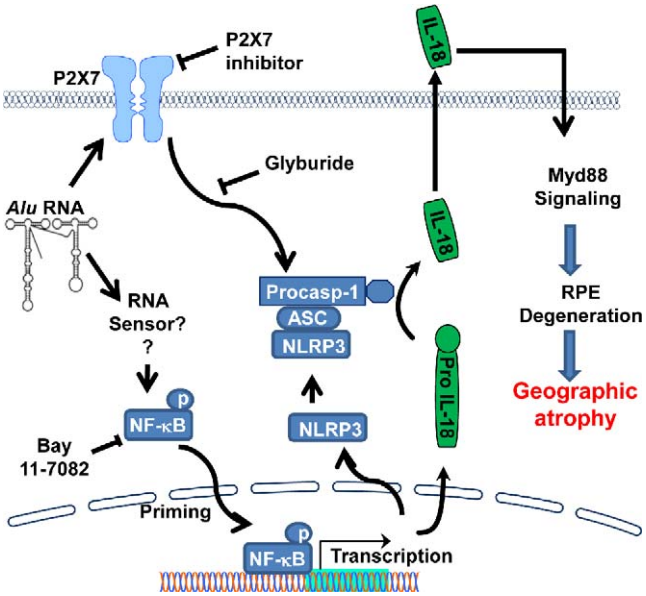

FIGURE 5. Schematic shows critical signaling pathways regulating NLRP3 priming and activation. *Alu* RNA-induced NF-κB-mediated transcriptional activation of inflammasome genes (NLRP3 and IL-18) and signaling via P2X7 receptors control NLRP3 inflammasome priming and activation, respectively. Identification of these key signaling events provides critical mechanistic insights into the recent implication of NLRP3 inflammasome activation and IL-18-induced Myd88 signaling in the pathogenesis of GA.[5]

(Fig. 4A, compare lanes 3 and 4). We found that intravitreous administration of the sulfonylurea glyburide, an NLRP3 inflammasome inhibitor acting downstream of P2X7 and upstream of NLRP3 inflammasome assembly,[18] protects against RPE degeneration induced by *Alu* RNA in WT mice (Fig. 4B). In contrast, glipizide, a related sulfonylurea that does not inhibit NLRP3, did not inhibit *Alu* RNA-induced RPE degeneration. We also observed that, intravitreous delivery of P2X7 inhibitor confers protection against the RPE degeneration induced by *Alu* RNA (Fig. 4C). Corroborating these findings, we also observed that *Alu* RNA did not induce RPE degeneration in *P2rx7*$^{-/-}$ mice (Fig. 4D). Collectively these findings suggest that P2X7 is an essential intermediate in *Alu* RNA-induced activation of NLRP3 inflammasome and consequent RPE degeneration.

DISCUSSION

Recently we reported that *Alu* RNA accumulation due to DICER1 deficiency induced RPE cell death via activation of the NLRP3 inflammasome.[5] The present study expands those findings and provides insight into the signaling pathways that regulate priming and activation of the NLRP3 inflammasome in the context of GA. Using both cell culture and mouse models, we demonstrated the critical importance of NF-κB and P2X7 in mediating *Alu* RNA-induced RPE degeneration.

NF-κB transcription factors play an important role in orchestrating host inflammatory and immune responses and modulate cellular growth properties by regulating the expression of specific set of cellular genes.[19] Similar to inflammasome activation by microbial pathogen-associated molecular patterns (PAMPs), LPS/ATP, toxins, and other triggers, *Alu* RNA-induced inflammasome priming/activation also depended on the NF-κB-mediated transcriptional activation of NLRP3 and IL-1 cytokines.[8,20,21] Assembly of the NLRP3 multiprotein scaffold is influenced by the integration of various proinflammatory signaling pathways. These proinflammatory pathways potentiate inflammasome priming through NF-κB-mediated induction of NLRP3 and IL-1 levels. Furthermore, *Alu* RNA-induced RPE degeneration was not observed in *Nfkb1*$^{-/-}$ mice, suggesting that NF-κB inhibition could be an attractive target for GA.

Most experimental protocols studying inflammasome activation use priming with TLR agonists such as LPS, which primes the NLRP3 inflammasome through NF-κB activation.[22–27] In the current model, *Alu* RNA-induced NLRP3 inflammasome priming and RPE degeneration are independent of TLR signaling. Our earlier studies demonstrated that other intracellular RNA sensors such as retinoic acid-inducible gene 1 (RIG-I), melanoma differentiation-associated protein 5 (MDA5), and protein kinase R (PKR) were also not required for *Alu* RNA-induced RPE degeneration.[5] In light of our present study, it appears that further studies are required to elucidate the precise sensor(s) of *Alu* RNA that enables its induction of NF-κB activation and NLRP3 priming.

The exact mechanism by which NLRP3 is activated remains elusive. Lysosomal destabilization, ROS production, and activation of P2X7 receptor are among the widely supported mechanisms.[7,8] Furthermore, the literature suggests that these pathways are not mutually exclusive.[7–11] In agreement with those studies, our findings with P2X7, combined with recent studies also implicating ROS in the *Alu* RNA-induced NLRP3 inflammasome activation, suggest that the complex interplay between ROS and P2X7 is critical for RPE degeneration in the context of *Alu* RNA cytotoxicity. P2X7 is a ligand-gated ion channel whose activation by high extracellular ATP leads to opening of ion channels that causes a decrease in intracellular K^+ levels, which in turn leads to NLRP3 activation.[7,28] Future studies will test whether *Alu* RNA also induces ATP release and K^+ efflux via P2X7.

Collectively, our studies provide greater insight into critical signaling pathways regulating *Alu* RNA-induced inflammasome activation and RPE degeneration (Fig. 5). Identification of NF-κB and P2X7 as critical signaling intermediates regulating *Alu* RNA-induced RPE degeneration suggests that targeting these pathways might be a useful strategy for rational drug development for treating GA. In addition, our data provide a rationale for testing glyburide, an agent widely used in treatment of type 2 diabetes, in treating GA. Glyburide is a functional inhibitor of ATP-sensitive potassium channels (K_{ATP}). Because the K_{ATP} channels in pancreatic β cells regulate the secretion of insulin, glyburide's inhibitory effect on K_{ATP} is exploited in the treatment of type 2 diabetes.[29] Interestingly, glyburide's ability to suppress NLRP3 activation is independent of its inhibitory effect on K_{ATP}, as glipizide, a related antidiabetic sulfonylurea drug that also potently blocks K_{ATP}, does not inhibit NLRP3.[18] Currently it is known only that glyburide acts upstream of NLRP3 and downstream of P2X7[18]; the precise molecular target of glyburide in inhibiting the NLRP3 inflammasome has yet to be identified.

Acknowledgments

The authors thank Charles Payne, Gary Pattison, Gregory Botzet, Robinette King, Li Xu, Darrell Robertson, Lindsay Toll, and Annette Uittenbogaard for technical assistance.

Supported by National Eye Institute/National Institutes of Health (NIH) Grants R01EY018350, R01EY018836, R01EY020672, and R01EY022238, a Doris Duke Distinguished Clinical Scientist Award, a Burroughs Wellcome Fund Clinical Scientist Award in Translational Research, an Ellison Medical Foundation Senior Scholar in Aging Award, the Dr. E. Vernon Smith and Eloise C. Smith Macular Degeneration Endowed Chair, the Carl Reeves Foundation, and Research to Prevent Blindness departmental

unrestricted grant (JA); by Beckman Initiative for Macular Research (NK); by Programme for Advanced Medical Education, sponsored by Fundação Calouste Gulbenkian, Fundação Champalimaud, Ministério da Saúde and Fundação para a Ciência e Tecnologia, Portugal (ABC); by American Heart Association and the National Center for Research Resources and the National Center for Advancing Translational Sciences, NIH, through Grant UL1TR000117 (BDG); by the Arnold and Mabel Beckman Foundation (DRH); and by NIH T32HL091812 and UL1RR033173 (BJF). The content of the article is the sole responsibility of the authors and does not necessarily represent the official views of the NIH.

Disclosure: **N. Kerur**, None; **Y. Hirano**, None; **V. Tarallo**, None; **B.J. Fowler**, None; **A. Bastos-Carvalho**, None; **T. Yasuma**, None; **R. Yasuma**, None; **Y. Kim**, None; **D.R. Hinton**, None; **C.J. Kirschning**, None; **B.D. Gelfand**, None; **J. Ambati**, P

References

1. Ambati J, Fowler BJ. Mechanisms of age-related macular degeneration. *Neuron*. 2012;75:26–39.
2. Bird AC. Therapeutic targets in age-related macular disease. *J Clin Invest*. 2010;120:3033–3041.
3. Ambati J, Atkinson JP, Gelfand BD. Immunology of age-related macular degeneration. *Nat Rev Immunol*. 2013;13:438–451.
4. Kaneko H, Dridi S, Tarallo V, et al. DICER1 deficit induces Alu RNA toxicity in age-related macular degeneration. *Nature*. 2011;471:325–330.
5. Tarallo V, Hirano Y, Gelfand BD, et al. DICER1 loss and Alu RNA induce age-related macular degeneration via the NLRP3 inflammasome and MyD88. *Cell*. 2012;149:847–859.
6. Cordaux R, Batzer MA. The impact of retrotransposons on human genome evolution. *Nat Rev Genet*. 2009;10:691–703.
7. Rathinam VA, Vanaja SK, Fitzgerald KA. Regulation of inflammasome signaling. *Nat Immunol*. 2012;13:333–342.
8. Schroder K, Tschopp J. The inflammasomes. *Cell*. 2010;140:821–832.
9. Bartlett R, Yerbury JJ, Sluyter R. P2X7 receptor activation induces reactive oxygen species formation and cell death in murine EOC13 microglia. *Mediators Inflamm*. 2013: 271813.
10. Cruz CM, Rinna A, Forman HJ, Ventura AL, Persechini PM, Ojcius DM. ATP activates a reactive oxygen species-dependent oxidative stress response and secretion of proinflammatory cytokines in macrophages. *J Biol Chem*. 2007;282:2871–2879.
11. Wang B, Sluyter R. P2X7 receptor activation induces reactive oxygen species formation in erythroid cells. *Purinergic Signal*. 2013;9:101–112.
12. Oldenburg M, Krüger A, Ferstl R, et al. TLR13 recognizes bacterial 23S rRNA devoid of erythromycin resistance-forming modification. *Science*. 2012;337:1111–1115.
13. Bennett EA, Keller H, Mills RE, et al. Active Alu retrotransposons in the human genome. *Genome Res*. 2008;18:1875–1883.
14. Shaikh TH, Roy AM, Kim J, Batzer MA, Deininger PL. cDNAs derived from primary and small cytoplasmic Alu (scAlu) transcripts. *J Mol Biol*. 1997;271:222–234.
15. Yang Z, Stratton C, Francis PJ, et al. Toll-like receptor 3 and geographic atrophy in age-related macular degeneration. *N Engle J Med*. 2008;359:1456–1463.
16. Yang P, Tyrrell J, Han I, Jaffe GJ. Expression and modulation of RPE cell membrane complement regulatory proteins. *Invest Ophthalmol Vis Sci*. 2009;50:3473–3481.
17. Akira S, Uematsu S, Takeuchi O. Pathogen recognition and innate immunity. *Cell*. 2006;124:783–801.
18. Lamkanfi M, Mueller JL, Vitari AC, et al. Glyburide inhibits the Cryopyrin/Nalp3 inflammasome. *J Cell Biol*. 2009;187:61–70.
19. Perkins ND. The Rel/NF-kappa B family: friend and foe. *Trends Biochem Sci*. 2000;25:434–440.
20. Kanneganti TD, Body-Malapel M, Amer A, et al. Critical role for Cryopyrin/Nalp3 in activation of caspase-1 in response to viral infection and double-stranded RNA. *J Biol Chem*. 2006;281:36560–36568.
21. Kanneganti TD, Ozören N, Body-Malapel M, et al. Bacterial RNA and small antiviral compounds activate caspase-1 through cryopyrin/Nalp3. *Nature*. 2006;440:233–236.
22. Cassel SL, Eisenbarth SC, Iyer SS, et al. The Nalp3 inflammasome is essential for the development of silicosis. *Proc Natl Acad Sci U S A*. 2008;105:9035–9040.
23. Dostert C, Pétrilli V, Van Bruggen R, Steele C, Mossman BT, Tschopp J. Innate immune activation through Nalp3 inflammasome sensing of asbestos and silica. *Science*. 2008;320:674–677.
24. Muruve DA, Pétrilli V, Zaiss AK, et al. The inflammasome recognizes cytosolic microbial and host DNA and triggers an innate immune response. *Nature*. 2008;452:103–107.
25. Halle A, Hornung V, Petzold GC, et al. The NALP3 inflammasome is involved in the innate immune response to amyloid-beta. *Nat Immunol*. 2008;9:857–865.
26. Martinon F, Petrilli V, Mayor A, Tardivel A, Tschopp J. Gout-associated uric acid crystals activate the NALP3 inflammasome. *Nature*. 2006;440:237–241.
27. Mariathasan S, Weiss DS, Newton K, et al. Cryopyrin activates the inflammasome in response to toxins and ATP. *Nature*. 2006;440:228–232.
28. Miller CM, Boulter NR, Fuller SJ, et al. The role of the P2X(7) receptor in infectious diseases. *PLoS Pathog*. 2011;7:e1002212.
29. Ashcroft FM. ATP-sensitive potassium channelopathies: focus on insulin secretion. *J Clin Invest*. 2005;115:2047–2058.

Investigative Ophthalmology & Visual Science